# DISPOSITIVI AD ATTRITO SOSTITUIBILI PER NODI DI TRAVI TRALICCIATE IN SOLUZIONE COMPOSTA ACCIAIO CALCESTRUZZO

# REPLACEABLE FRICTION DEVICE FOR STEEL-CONCRETE COMPOSITE TRUSSED BEAM-TO-RC COLUMN JOINT

Salvatore Pagnotta, Muhammad Ahmed,
Piero Colajanni, Lidia La Mendola
University of Palermo
Department of Engineering
Palermo, Italy
salvatore.pagnotta@unipa.it,
muhammad.ahmed@unipa.it
piero.colajanni@unipa.it
lidia.lamendola@unipa.it

Alessia Monaco
Politecnico di Torino
Department of Architecture and Design
Turin, Italy
alessia.monaco@polito.it

## ABSTRACT

During the last years, earthquake-resilient Moment-Resisting Frames (MRFs) structures have become increasingly popular thanks to their ability of limiting the damage experienced by surrounding structural and non-structural members. Within this framework, few solutions have been proposed for cast-in-situ steel-concrete composite structures, being challenging to develop earthquake-proof low-cost beam-to-column connections. This issue can be solved by using the structural typology of the Hybrid Steel-Trussed Concrete Beams (HSTCB). These are usually design to cover long spans with a small height, leading to a large amount of rebars, which, passing through small beam-column joints, make the latter more easily damageable if subjected to an earthquake. The introduction of friction devices at the Beam-to-Column Connections (BCCs) can help to lengthen the lever arm of the moment transferred between beam and column, thus decreasing the shear force acting on the RC joint preventing its damage. In this context, this paper focuses on a new BCC developed for RC MRFs made with HSTCBs, which is endowed with a replaceable friction device. The main features of the proposed solution and its design procedure are outlined. After that, a comprehensive 3D finite element model of the proposed solution is developed. Monotonic and cyclic analyses are carried out considering several sliding moment values. The results prove that the proposed connection is able not only to provide adequate dissipative capacity, but also to avoid damaging of surrounding RC members.

## SOMMARIO

Negli ultimi anni, le strutture intelaiate sismo-resilienti sono diventate sempre più popolari grazie alla loro capacità di limitare i danni subiti dagli elementi strutturali e non strutturali. In questo contesto, poche soluzioni sono state proposte per le strutture composte acciaio-calcestruzzo gettate in opera, in quanto lo sviluppo di connessioni trave-colonna economiche ed a basso danneggiamento risulta complesso. La tipologia strutturale delle travi ibride acciaio-calcestruzzo (HSTCB) può essere una valida soluzione per la risoluzione del suddetto problema. Infatti, queste travi sono solitamente progettate per coprire lunghe campate con un'altezza ridotta, il che porta ad una grande quantità di armature nelle zone d'estremità che, passando attraverso nodi trave-colonna di ridotte dimensioni, rende questi ultimi più facilmente danneggiabili se sottoposti ad un terremoto. L'introduzione di dispositivi ad attrito nelle connessioni trave-colonna (BCC) permette di allungare il braccio di leva del momento trasferito tra trave e colonna, diminuendo così la forza di taglio che agisce sul nodo in c.a. evitandone il danneggiamento. In questo contesto, il presente lavoro si concentra su una nuova connessione trave-colonna sviluppata per sistemi intelaiati in c.a. realizzati mediante travi HSTCB, queste ultime dotate di dispositive sostituibili di attrito. Inizialmente, vengono delineate le caratteristiche principali della soluzione proposta e la sua procedura di progettazione. Successivamente, viene sviluppato un modello dettagliato agli elementi finiti 3D della soluzione proposta, col quale sono eseguite sia analisi monotoniche che cicliche, considerando diversi valori di progetto del momento che porta allo scorrimento del dispositivo. I risultati dimostrano che la connessione proposta è in grado non solo di fornire un'adeguata capacità dissipativa, ma anche di evitare il danneggiamento degli elementi in c.a. circostanti.


## 1 INTRODUCTION

Over the past three decades, engineers and researchers have been trying to develop a design technique in order to mitigate the structural damage induce to the building due to earthquakes. The main purpose of such research is to develop a design technique or to develop such a mechanism that buildings and structures dissipate the energy, the damage should be less or after experiencing the cyclic loads the building becomes functional as soon as possible. Keeping the purpose in mind and analyzing the solutions that have been developed for moment-resisting frames (MRFs), some devices are designed which can be used at the Beam-to-Column Connection (BCC) of steel structure named the Removable Friction Dampers [1] and the Sliding Hinge Joint [2]. However, fewer devices have been developed for RC structures especially for cast-in-place members due to factors like design difficulties in making economical yet damage-proof connections [3,4]. Hybrid Steel-Trussed Concrete Beam (HSTCB) together with friction BCC is one of the effective solutions. HSTCB can be easily equipped with a friction device because the bottom steel plate of HSTCB is similar to that of a structural steel member. HSTCBs have a smaller effective depth which leads to a large number of longitudinal bars, these bars are more prone to damage due to cyclic loadings if pass through a small beam to column joint. To mitigate it, in this paper structural configuration of the friction-based beam to column connection made with HSTCBs is discussed. The proposed model is designed in such a way to increase the lever arm of the moments transferred between the beam and joint. Due to this, the shear force at the panel zone decreases significantly. In this paper first of all the model is described comprehensively focusing on its distinguishing features followed by the design procedure of friction based BCCs. Later, a detailed 3D finite element model of the exterior beam to column joint together with the proposed connection is developed. To investigate the functionality of the model under different design moment values several cyclic and monotonic analyses are performed. In the end, the numerical results are discussed which confirms the efficiency of the model in reducing the damage in beam to column joint and in energy dissipation. Analyses give wide and stable hysteresis loops which confirms the flexural behaviour of the model.

## 2 PROPOSED BEAM TO COLUMN CONNECTION

The proposed beam-to-column connection can be applied to any type of beam and column having any type of geometrical and mechanical characteristics. To develop a connection, beams, and columns with similar properties as of [5] are taken. The cross-sectional dimensions of beams and columns are taken as 300 x 250 mm and 400 x 300 mm respectively. The longitudinal reinforcement for beam and column is taken as 4ϕ24 (top) + 2ϕ24 (bottom) and 10ϕ20 respectively. Shear reinforcement for the beam is taken as ϕ8/6 cm while for the column it's taken as ϕ8/11 cm. The web truss of HSTCB has 2ϕ12 inclined bars with 300 mm spacings while a bottom plate is taken as 5 mm thick. Further explanation of the proposed connection (Fig. 1.) is given below: the bottom side of the horizontal plate (top green) is welded with the central plate while its top side is welded with longitudinal reinforcement of the HSTCB; T stub in cyan colour is connected to the columns with threaded bars passing through it while it is connected to the top horizontal plate by using an ordinary bolted friction connection; studs are shown in yellow colour which connects the bottom plate of the steel truss to the top horizontal plate; a friction device made with the central plate (red) and two steel angles (blue) is at the bottom part of the beam while these elements are connected using preloaded bolts which pass through curved slotted holes in the central plate; perfonond connectors are made on the top horizontal plate and central plate whose purpose is to ensure the connection between concrete core of the beam and steel elements.

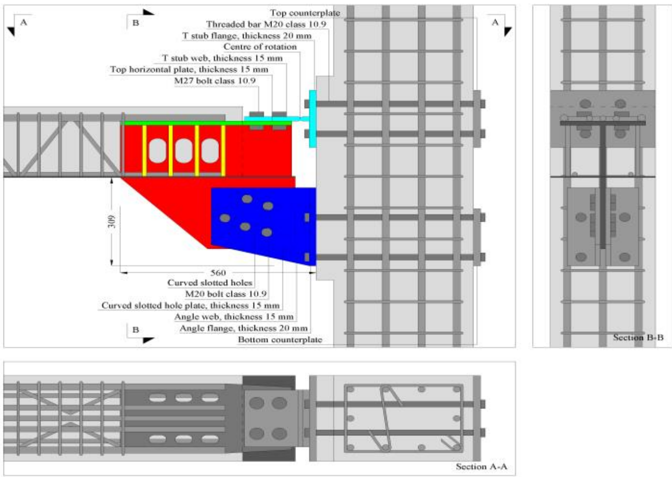


**Fig. 1.** The proposed beam to column connection

The connection proposed in [6] and [7] have inadequate mechanical performance due to insufficient stiffness of beam to column connection and due to the complex construction process. The aim is to improve the mechanical performance of the connection proposed in [6,7]. To enhance its performance top horizontal and vertical central plates are used. The connection is designed in a way to rotate around the centre of rotation located near the base section of the T stub. Curved slotted holes are used to prevent the hitting of bolts with the central plate during the sliding phase. So, by using this technique, the only friction force arises due to the friction device. Thus, the moment capacity of connection remains constant during the sliding of the device and a reduction in over strengthening factor could be possible which ultimately reduces the construction cost.

## 3 DESIGN METHOD

Firstly, a design moment is to be defined which initiates the sliding of the device. In this example, the connection is designed for the RC frame having 6m of height (two stories of 3m each) and two bays of 5m width each. The dimensions and reinforcement of beams and columns are as same as described in previous Section 2. More details about the properties of the RC frame can be found in [8]. The hogging moment strength $M_{Rd}$ of the beam used in the RC frame, according to the previous section is 165kNm. The overstrength factor is taken as 1.5 and thus the design moment $M_d$ is calculated as $M_{Rd} / \Omega_\mu$ = 165 / 1.5 = 110 kNm. The aim of the overstrength factor is to avoid any damage to the reinforced concrete member around the proposed connection. The values of over strength factor are taken as suggested by some other research groups ($\Omega_\mu$ = 2 in [1], $\Omega_\mu$ = 1.4 in [2]). The force which needs to slide the device $F_d$ can be evaluated as follow:

$$F_d = M_d / z = 110 / 0.375 = 294\ kN \tag{1}$$

In equation 1, $z$ represents the lever arm which is taken as 1.5 times the cross-sectional height of the HSTCB. 5 M20 bolts class 10.9 arranged in two rows are used in the friction device. To minimize the long-term and short-term loss of preload acting on the bolts the preload is kept within a limit of 30-60% of the values suggested by [1] and mentioned in EN1993-1-8 [9]. Now, the sliding force can be calculated as follow:

$$F_d = t_s n_b n_s \mu F_{pc,M20} \tag{2}$$

In equation (2), $n_s$ represents the number of surfaces on which the friction forces are generated, $n_b$ represents the number of bolts (5), $\mu$ is the coefficient of friction (0.4), $F_{pc,M20}$ represents the preloading force according to EN1993-1-8 which in our case is (171.5 kN), while $t_s$ is the ratio between the effective preload of the bolt and the value consistent with the code.

By using equation (1) and equation (2) the value of $t_s$ can be calculated as 0.429. The horizontal and vertical components of the forces acting on steel angles and T stub can be calculated as follows:

$$F_{d,v} = \Omega_\mu F_d \cos(\alpha) = 165\ kN \qquad F_{d,h} = \Omega_\mu F_d \sin(\alpha) = 409\ kN \tag{3}$$

In equation 3, $\alpha$ is the angle between the axis connecting the point of application of $B$ of the $F_d$ with the axis connecting the centre of rotation $A$ and the axis of the HSTCB.

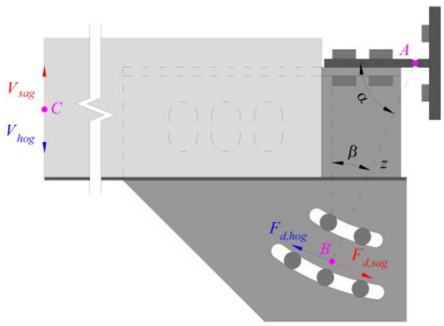


**Fig. 2.** Forces acting on the HSTCB computing the equilibrium with respect to point A

## 4 DETAILS OF THE FINITE ELEMENT MODEL

The finite element model was developed by using the ABAQUS/CAE software. The model is able to consider the geometrical and material nonlinearities. To deeply analyze the linkage between the steel elements (which composes the HSTCB) and the concrete core of the beam, both shear and longitudinal reinforcements were modelled as a three-dimensional (3D) element. The interaction property between the concrete and these steel elements was taken as cohesive to simulate the bond stress-slip behaviour. 8-node linear brick elements were used to model all elements of the connection, while for the HSTCB and steel truss 4-node linear tetrahedron (C3D4) was used. Column rebars were modelled using a 2-node beam element (B3D2), while the interaction between the column rebars and the concrete of the column was simulated by means of the embedded constraint. Mesh size is taken as 30 mm for steel truss, 10 mm for steel angles and T stub, 5 mm for bolts and 40 mm for beam and column as shown in (Fig. 3.). The assumptions for the development of the finite element model are taken according to the one proposed in [7] and [10] in order to reproduce the shear and flexural behaviour of HSTB, as well as the mechanical performance of friction devices, which were correctly verified against experimental results. The developed model reproduces an exterior beam to column joint, the length of the beam is considered 2.73m while the column height is considered 3 m. The distance between the beam end and the centre of rotation (*L*) is taken as 2.635 m. The longitudinal and shear reinforcement of beam and column, as well as their cross-sectional dimensions, are reported in [5] and Section 2. An analytical method which is able to calculate the shear strength of the beam with two different orders of transverse reinforcement is used to evaluate the shear strength of the beam [11]. According to this model, the shear strength of HSTCB is calculated as 350 kN, while the maximum shear force on the beam can be calculated as $V_{Sd} = \Omega_\mu M_d / L$ = 63 kN, which is quite less than the shear strength of HSTCB. The concrete damaged plasticity model was used to simulate the mechanical behaviour of concrete. The equations of [12] were used to calculate the compressive stress-strain relationship. The cylindrical compressive strength is considered as 30.31 Mpa and strain at peak value as 0.002, which is consistent with the values reported in [5]. The concrete was considered elastic before achieving the tensile strength (2.57 Mpa). The post-peak behaviour was simulated by using the fracture energy method and it was calculated as recommended by CEB-FIP Model Code (2010) [13] and equal to $G_F$ = 0.13 N/mm. Table 1 shows the values of the parameters which were used in the CDP model.

**Table 1.** Parameters used in CDP model

| CDP parameters | | | | |
|---|---|---|---|---|
| Dilation angle | K | Viscosity | Eccentricity | $f_{b0}/f_{c0}$ |
| 40 | 0.67 | 0.0001 | 0.1 | 1.16 |

For steel elements, different stress-strain curves were used depending on each steel grade. The model proposed in [14] was used considering a quad-linear stress-strain relationship to model the mechanical behaviour of elements and rebars made of constructional steel. As consistent with [5], the yielding stresses were set as 500 MPa and 400 MPa respectively. The model proposed in [15] was used for threaded bolts and bars which enabled us to take into account the additional deformability given by a threaded length. To model, the bar-slip mechanism between rebars and concrete of the beam a cohesive interaction approach is adopted [16]. Coulomb model of friction was used for modelling the interaction between steel elements using the friction coefficient of 0.2. While for the interaction between the lower part of the vertical central plate and steel angles the friction coefficient is taken as 0.4. The model analysis is further divided into three steps: 1) bolt preloading; 2) applying axial load on the column; 3) imposing displacement at the column base. Boundary conditions and load application is illustrated in Fig. 3. The beam end section is constrained with a roller while the top and base of the column are constrained by a hinge and roller respectively. In the third step, the hinge applied to the column top section is activated. As the interactions are quite higher which results in convergence issues so, in order to solve them a contact control is used. It is used on the interactions involving the threaded bars passing through the column, activated only during the first step. The contact control option is used to help the contact initiation between several elements in which rigid body motions are not constrained. The automatic stabilization option "Specify dissipated energy fraction" is used, set to the default value of 0.0002. Two groups of monotonic analyses were performed by applying a displacement of 270 mm to the column base, leftward for the first group while rightward for the second group. To simulate different values of design moments ($M_d$ and 1.5 $M_d$), two analyses were performed on each group considering different preloading forces acting on the bolts of the friction device. Then, after changing bolt preload two cyclic analyses were performed. The moment acting on the friction joint is computed by the product of vertical force on the beam and the distance between the assumed centre of rotation and beam end section (2.635 m). The loading protocol of the cyclic analyses was defined on the basis of the yielding chord rotation of the monotonic analysis with $M_d$ = 110 kNm, equal to $\theta_y$ = 7 mrad. Three cycles were defined, characterized by amplitudes of ± $\theta_y$, ± 4$\theta_y$ and ± 7$\theta_y$. The loading protocol of the cyclic analyses was defined based on the yielding chord rotation of the monotonic analysis with $M_d$ = 110 kNm, equal to $\theta_y$ = 7 mrad. Three cycles were defined, of amplitudes ± $\theta_y$, ± 4$\theta_y$ and ± 7$\theta_y$.

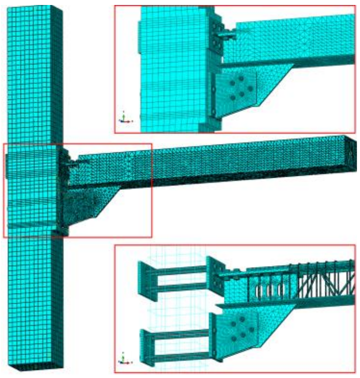

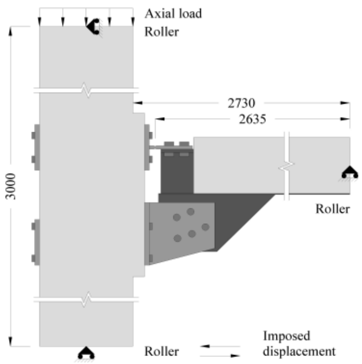


**Fig. 3.** Meshed FE model (left). Loads and boundary conditions of the FE model (right)

## 5 RESULTS OF THE FINITE ELEMENT ANALYSES

### 5.1 Monotonic Behaviour of the Model

The monotonic moment chord rotation curves are demonstrated in the Fig. 4. given below.
It can be analyzed from the figure that the yielding moments and analytical moments have quite near values. It can be seen that analytical yielding moments are 2-3% less than the hogging moments, while analytical yielding moments are 10-12% higher than sagging moments. The curves also show three phases which are: the first one shows that the device does not slip because of the elastic response; the second one is the one where the sliding of friction device occurs and the overall response is thus perfectly-plastic; the third phase is where the bolt shanks strike with

the end section of curved slotted holes and the rotation is higher than the design rotation (50 mrad).

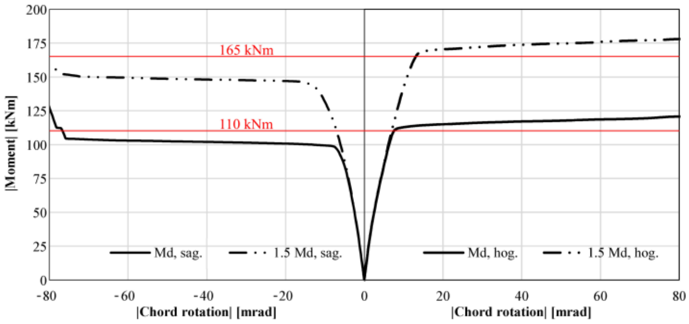


**Fig. 4.** Monotonic analyses: moment-chord rotation curves

From these results, it can be analyzed that there is sufficient stiffness of all the elements of the connection because of which the connection doesn't shift during sliding, and it rotates around the assumed centre of rotation perfectly. For $M_d$ = 165 kNm, (Fig.5. left) shows the stress state acting on the steel element when the chord rotation is 70mrad for hogging and (Fig.5. right) shows it for sagging. All the steel elements are characterized by stresses which are lower than the yielding values, proving the efficiency of the design procedure. It can be analyzed that for the hogging moment the longitudinal reinforcement has stresses near 500 Mpa, which actually is the yielding stress. More stress values can be seen on the T stub at the section where it is expected the formation of a plastic hinge act as centre of rotation. For $M_d$ = 165 kNm, (Fig.6. left) shows minimum principal stresses acting on the concrete when the chord rotation is 70mrad for hogging and (Fig.6. right) shows it for sagging. Generally, it can be seen that the device is able to mitigate the damage to concrete, prevents reduction in stiffness and strength of connection and limits the compressive stresses in beam, column and beam-to-column joint panel. But it can also be seen that there is a higher value of minimum principal stresses than the compressive strength of concrete in particular areas, because of the biaxial or triaxial state of stresses which are acting in such areas.

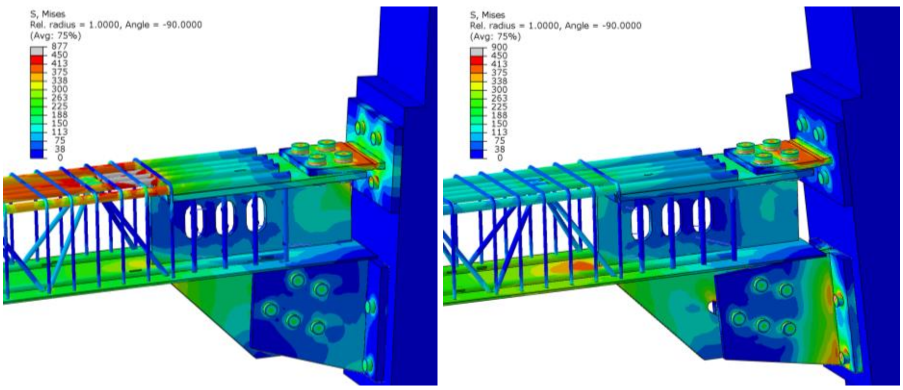


**Fig. 5.** For $M_d$ = 165 kNm, stress values acting on the steel elements at the chord rotation of 70 mrad for hogging (left) and sagging (right)

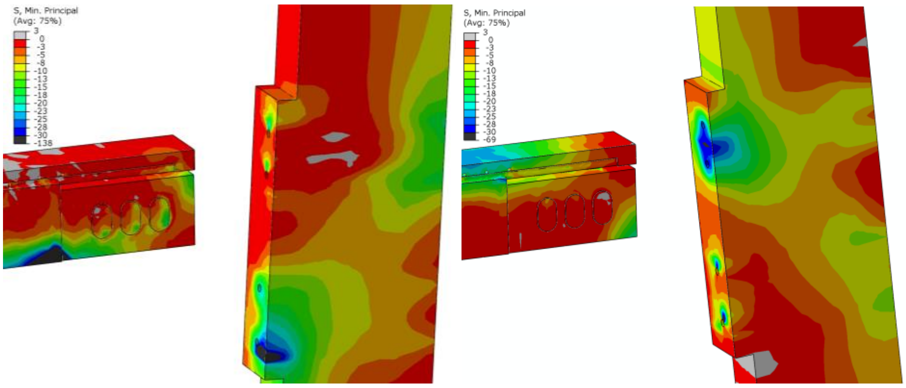


**Fig. 6.** For $M_d$ = 165 kNm, minimum principal stresses in concrete members at the chord rotation of 70 mrad for hogging (left) and sagging (right)

## 5.2 Cyclic Behaviour of the Model

Fig. 7. shows the curves of moment chord rotation which are obtained with the cyclic analyses. It can be seen that the hysteresis loops obtained are quite stable and wide there is proportionality between the response of the system and the preload acting on the bolts.

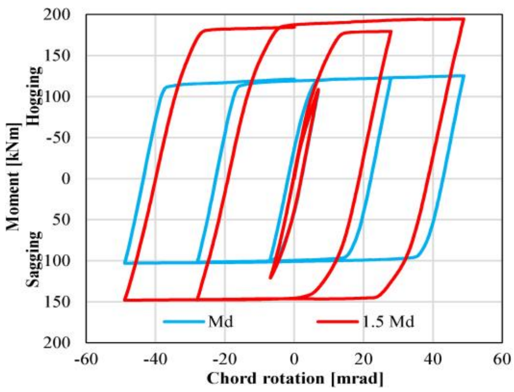


**Fig. 7.** Cyclic analyses: moment-chord rotation curves

Fig. 8. shows the equivalent plastic strains which are taken by the steel elements at the end of cyclic analysis when the design moment is 165kNm. It can be analyzed from the analysis that the T stub experiences plastic deformation that is extended toward the nearest row of bolts. It means that during the cyclic analysis there is a shifting of the centre of rotation. However, due to this phenomenon, there isn't much influence on the overall response of the connection. It is also observed that there are some plasticization's on the longitudinal reinforcement near the area of the bottom plate adjacent/next to the inner side of the vertical central plate and near the connection of the top horizontal plate. Fig. 8 (right) shows the equivalent plastic tensile strains of concrete at the end of cyclic analysis when the design moment is 165kNm. It is revealed from the analysis that there are some cracks on the concrete members. Some of them are: cracks around the dowel of perfobound connectors, horizontal cracks on columns, near the connection with threaded bars, due

to compressive/tensile forces shifted by steel angles and T stub and some vertical cracks also observed at the inner side of the vertical central plate. These cracks are an efficiency check which confirms that the system is well integrated and there is a proper connection of steel elements with the concrete core. Fig. 7. also confirms that despite these cracks there isn't a notable effect on the overall response of the connection. No diagonal cracks observed on the joint panel which proves that the proposed model is able to meet the design expectations i.e., to ensure the mechanical performance and to significantly reduce the damage at the joint panel.

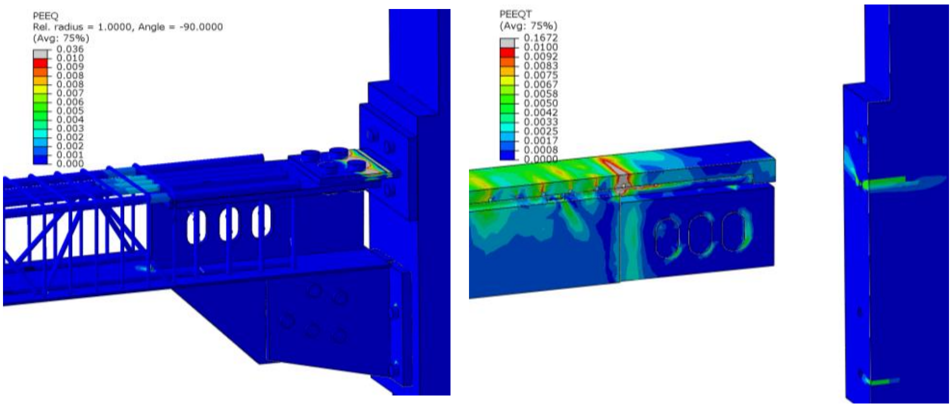


**Fig. 8.** At the end of the cyclic test for $M_d$ = 165 kNm, equivalent plastic strain of steel elements (left), equivalent plastic tensile strain of concrete (right)

## ACKNOWLEDGEMENTS

The economic support to the research of the SICILFERRO TORRENOVESE s.r.l. company is acknowledged, and the Authors thank Dr. Mauro Scurria and Eng. Nicolò Cancelliere for helpful discussion and active participation in the research project.

## REFERENCES

[1] Latour, Massimo, Mario D'Aniello, Mariana Zimbru, Gianvittorio Rizzano, Vincenzo Piluso, and Raffaele Landolfo. 2018. "Removable friction dampers for low-damage steel beam-to-column joint." *Soil Dynamics and Earthquake Engineering* 115:66-81. Accessed December 21, 2020. doi: 10.1016/j.soildyn.2018.08.002.

[2] Khoo, Hsen-Han, Charles Clifton, Gregory MacRae, Hao Zhou, and Shahab Ramhormozian. 2015. "Proposed design models for the asymmetric friction connection." *Earthquake Engineering and Structural Dynamics* 44:1309-24. Accessed January 9, 2021. doi:10.1002/eqe.2520.

[3] Morgen, Brian G., and Yahya C. Kurama. 2004. "A friction damper for post-tensioned precast concrete moment frames." *PCI Journal* 49:112-33. Accessed November 2, 2020. doi:10.15554/pcij.07012004.112.133.

[4] Tsampras, Georgios, Richard Sause, Robert B. Fleischman, and José I. Restrepo. 2018 "Experimental study of deformable connection consisting of friction device and rubber bearings to connect floor system to lateral force resisting system." *Earthquake Engineering and Structural Dynamics* 47:1032-53. Accessed December 5, 2020. doi:10.1002/eqe.3004.

[5] Colajanni, Piero, Lidia La Mendola, Alessia Monaco, and Nino Spinella. 2016. "Cyclic behavior of composite truss beam-to-RC column joints in MRFs." *Key Engineering Materials* 711:681-9. Accessed January 19, 2021. doi:10.4028/www.scientific.net/KEM.711.681.

[6] Colajanni, Piero, Lidia La Mendola, Alessia Monaco, and Salvatore Pagnotta. 2020. "Dissipative connections of rc frames with prefabricated steel-trussed-concrete beams." *Ingegneria Sismica* 37:51-63. Accessed March 08, 2021. http://ingegneriasismica.org/product/5-2020-1-dissipative-connections-of-rc-frames-with-prefabricated-steel-trussed-concrete-beams.

[7] Colajanni, Piero, Lidia La Mendola, Alessia Monaco, and Salvatore Pagnotta. 2021. "Design of RC joints equipped with hybrid trussed beams and friction dampers." *Engineering Structures* 227:111442. Accessed April 14, 2021. doi:10.1016/j.engstruct.2020.111442.

[8] Colajanni, Piero, Lidia La Mendola, Alessia Monaco, and Salvatore Pagnotta. 2021. "Seismic performance of earthquake-resilient RC frames made with HSTC beams and friction damper devices." *Journal of Earthquake Engineering* Article in press. doi:10.1080/13632469.2021.1964652.

[9] EN 1993:1-8, Design of steel structures – Part 1-8: design of joints, CEN, 2005.

[10] Ballarini, Roberto, Lidia La Mendola, Jia-Liang Le, and Alessia Monaco. 2017. "Computational study of failure of hybrid steel trussed concrete beams." *Journal of Structural Engineering* 143:04017060. Accessed October 31, 2020. doi: 10.1061/(ASCE)ST.1943-541X.0001792.

[11] Colajanni, Piero, Salvatore Pagnotta, Antonino Recupero, and Nino Spinella. 2020. "Shear resistance analytical evaluation for RC beams with transverse reinforcement with two different inclinations." Materials and Structures 53:18. doi:10.1617/s11527-020-1452-8.

[12] Saenz, L. P. 1964. "Discussion of "Equation for the stress-strain curve of concrete," by Desayi and Krishnan." *ACI Journal* 61:1229-35. Accessed January 4, 2021.

[13] Ceb-Fip Model Code 2010, Comité Euro-International du Béton, Lausanne, Switzerland, 2010

[14] Yun, Xiang, and Leroy Gardner. 2017. "Stress-strain curves for hot-rolled steels." *Journal of Constructional Steel Research* 133:36-46. Accessed February 4, 2021. doi:10.1016/j.jcsr.2017.01.024.

[15] D'Aniello, Mario, David Cassiano, and Raffaele Landolfo. 2017. "Simplified criteria for finite element modelling of European preloadable bolts." Steel and Composite Structures 24:643-658. Accessed February 27, 2021. doi:10.12989/scs.2017.24.6.643.

[16] Eligehausen, Rolf, Egor P. Popov, and Vitelmo V. Bertero. 1983. "Local bond stress-slip relationships of deformed bars under generalized excitations." UCB/EERC-83/23, College of Engineering, University of California, Berkeley, CA. Accessed April 15, 2021.

## KEYWORDS

Earthquake-resilient structures; friction device; hybrid steel-trussed concrete beam; reinforced concrete.